Zero Phase Difference Capacitance Control (ZPDCC) for Magnetically Resonant Wireless Power Transmission

Shunta Iguchi, Pyungwoo Yeon, Hiroshi Fuketa, Koichi Ishida, Takayasu Sakurai, and Makato Takamiya
University of Tokyo, 4-6-1 Komaba, Meguro-ku, Tokyo 153-8505, Japan

***Abstract*- In a magnetically resonant wireless power transmission system, a DC-DC power transmission efficiency (η_{TOTAL}) at an inherent resonant frequency (f_{RES}) is degraded when the distance between a transmitter (TX) coil and a receiver (RX) coil is short, because the frequency dependence of η_{TOTAL} has two peaks. In order to solve the efficiency degradation, a zero phase difference capacitance control (ZPDCC) is proposed, which is suitable for the integration to LSI's. In ZPDCC, either of the two peaks is shifted to f_{RES} and η_{TOTAL} is increased by tuning the capacitance (C) of the resonator in TX and RX to keep the zero phase difference ($\theta = 0$) between the voltage and the current in TX at $\Delta\theta / \Delta C > 0$. Both TX and RX circuits are fabricated in a 3.3V, 180nm CMOS. By introducing ZPDCC, the measured η_{TOTAL} at f_{RES} of 13.56MHz increases 1.7 times from 16% to 27% at the distance of 2.5mm between the TX and RX coils with a diameter of 40mm.**

I. Introduction

Ambient or ubiquitous charging of electronic devices such as smartphones is increasingly needed, because the smartphone requires a frequent charging due to the increased power consumption. A magnetically resonant wireless power transmission board (MR-WPTB) [1] on a printed-circuit board (PCB) with a transmitter (TX) coil array and a selectively activation of a TX coil based on the position detection of a receiver (RX) coil is one of a possible solution for the ambient charging.

In MR-WPTB, however, a DC-DC power transmission efficiency (η_{TOTAL}) at an inherent resonant frequency (f_{RES}) including a power amplifier (PA) in TX and a rectifier in RX reaches its maximum at a certain distance (d_X) between a TX coil and a RX coil. When the distance (d) between a TX coil and a RX coil is shorter than d_X, η_{TOTAL} at f_{RES} is reduced, which is a unique phenomenon in the magnetic resonance [1] and is not observed in the conventional electromagnetic induction.

In order to solve the efficiency reduction in the magnetic resonance, a zero phase difference capacitance control (ZPDCC) is proposed in this paper, which is suitable for the integration to LSI's. By introducing ZPDCC, η_{TOTAL} at f_{RES} is increased.

II. Zero Phase Difference Capacitance Control (ZPDCC)

In order to analyze the frequency dependence of η_{TOTAL}, Fig. 1 shows a schematic of a magnetically resonant wireless power transmission system including PA and a rectifier. The details of the circuits of a class-D PA and the rectifier will be shown in Fig. 4. P_1 is an input power to TX, P_2 is an output power of PA, P_3 is an input power to the rectifier, and P_4 is a load power. P_1, P_2, P_3, and P_4 are effective powers. The definitions of a PA efficiency (η_{PA}), a coil efficiency (η_{COIL}), a rectifier efficiency ($\eta_{RECTIFIER}$), and η_{TOTAL} are shown in Fig. 1.

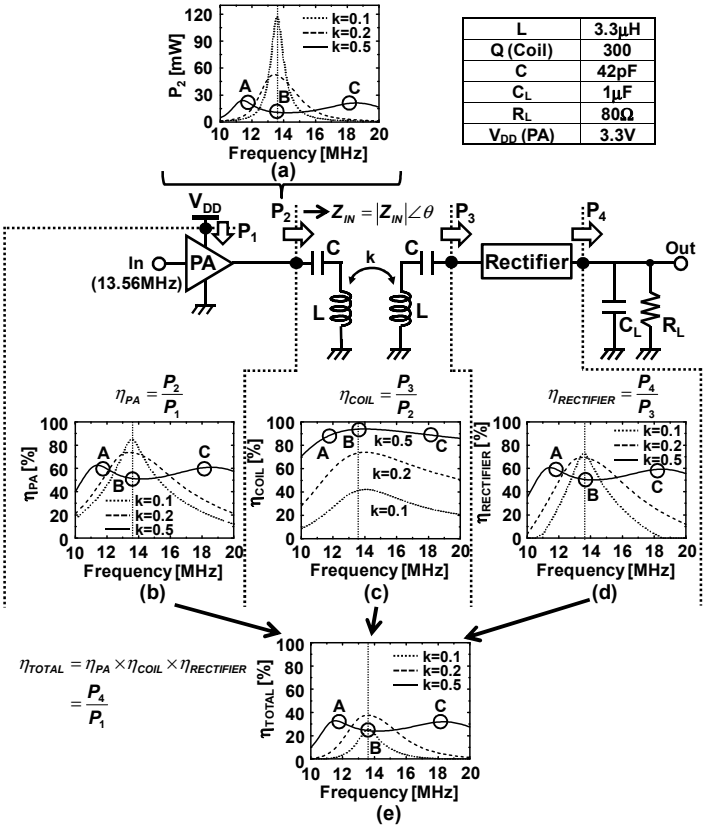

Fig. 1. Schematic of magnetically resonant wireless power transmission system. Simulated frequency dependence of (a) P_2, (b) η_{PA}, (c) η_{COIL}, (d) $\eta_{RECTIFIER}$, and (e) η_{TOTAL}. Coupling coefficient (k) is varied.

Fig. 1 (a) shows a simulated frequency dependence of P_2. Figs. 1 (b) - (e) show simulated frequency dependence of η_{PA}, η_{COIL}, $\eta_{RECTIFIER}$, and η_{TOTAL}, respectively. A coupling coefficient (k) is varied to emulate the change of d. In the SPICE simulation, a 3.3V, 180nm CMOS is used with the parameters in the table in Fig. 1. In this work, the target frequency is fixed to 13.56MHz.

The frequency dependence of the efficiency, one peak or two peaks, is discussed in the followings. The frequency

dependence of η_{COIL} has the one peak [2]. In contrast, the frequency dependences of η_{PA}, $\eta_{RECTIFIER}$, and η_{TOTAL} have the two peaks. The origin of the two peaks derives from the two peaks of P_2 shown in Fig. 1 (a). The reason is explained in the next paragraph. The frequency dependence of η_{PA} has the two peaks, because η_{PA} increases with increasing P_2. Similarly, the frequency dependence of $\eta_{RECTIFIER}$ has the two peaks, because $\eta_{RECTIFIER}$ increases with increasing P_3. Therefore, the frequency dependence of η_{TOTAL} (= η_{PA} x η_{COIL} x $\eta_{RECTIFIER}$) has the two peaks.

The reason why the frequency dependence of P_2 has the two peaks is explained in the following. P_2 of class-D PA is given by [3]

$$P_2 = \frac{2V_{DD}{}^2 \cos^2(\theta)}{\pi^2 \,\mathrm{Re}(Z_{IN})} \qquad (1)$$

where V_{DD} is a power supply voltage of PA, Z_{IN} is an input impedance at the coil as shown in Fig. 1, θ is a phase of Z_{IN}, and π is a circular constant. P_2 is determined by θ and Re(Z_{IN}), because V_{DD} is fixed to 3.3V in this work. P_2 is maximized, when $\theta = 0$ and Re(Z_{IN}) is minimum. Figs. 2 (a) and (b) show simulated frequency dependence of θ and Re(Z_{IN}), respectively. k and the capacitance (C) of the resonator in TX and RX shown in Fig. 1 are varied. In Fig. 2 (a) at $k = 0.1$, the frequency at $\theta = 0$ is only 13.56MHz, which corresponds to the one peak in Fig. 1 (a). In contrast, in Fig. 2 (a) at $k = 0.5$ and C = 42pF, the frequencies at $\theta = 0$ are Point A, Point B, Point C shown in Fig. 2 (a). Point B is 13.56MHz. Point A and Point C corresponds to the two peaks in Fig. 1 (a) and Point B corresponds to a bottom of a valley in Fig. 1 (a), because Re(Z_{IN}) of Point A and Point C is smaller than Re(Z_{IN}) of Point B. In this way, the frequency dependence of P_2 has the two peaks in Fig. 1 (a).

In this paper, in order to increase η_{TOTAL} at k = 0.5 and 13.56MHz shown as Point B in Fig. 1 (e), Point A or Point C is moved to 13.56MHz by changing C. In order to determine an optimum C, ZPDCC is proposed. In ZPDCC, C is tuned to keep $\theta = 0$ at $\Delta\theta / \Delta C > 0$, thereby shifting either of Point A or Point C to 13.56MHz and increasing η_{TOTAL}. For example, when C is changed from 42pF to 31pF at $k = 0.5$, Point A moves to Point D (= 13.56MHz) as shown in Fig. 2 (a) and Re(Z_{IN}) at 13.56MHz decreases from Point B to Point D as shown in Fig. 2 (b), thereby increasing P_2 and η_{TOTAL}.

The reason why $\theta = 0$ at $\Delta\theta / \Delta C > 0$ is required in ZPDCC is explained in the following. Figs. 3 (a) and (b) show simulated capacitance (C) dependence of θ and Re(Z_{IN}) at k = 0.5 and 13.56MHz, respectively. In Fig. 3 (a), C at $\theta = 0$ are Point B, Point D, and Point E. In Fig. 3 (b), Re(Z_{IN}) at Point D and Point E is smaller than Re(Z_{IN}) at Point B. Therefore, P_2 and η_{TOTAL} at Point D and Point E is larger than those at Point B. For ZPDCC, Point D and Point E are right points, while Point B is a wrong point. In order to distinguish Point D and Point E from Point B, " $\Delta\theta / \Delta C > 0$" condition is required. In this work, Point B is moved to Point D by changing C from 42pF to 31pF.

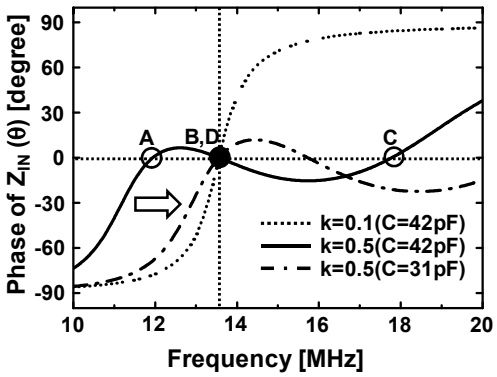

(a)

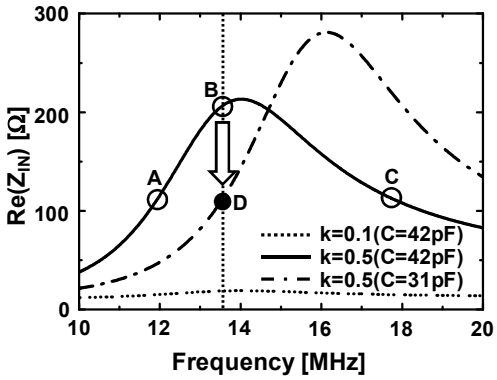

(b)

Fig. 2. Simulated frequency dependence of (a) θ and (b) Re(Z_{IN}). k and C are varied.

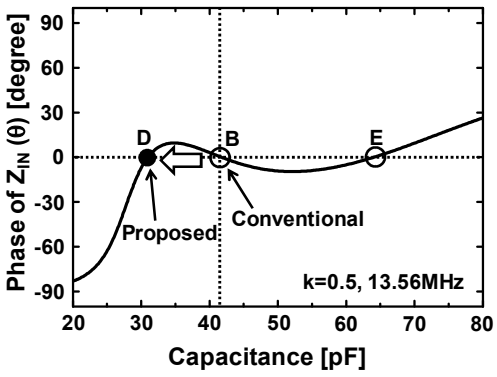

(a)

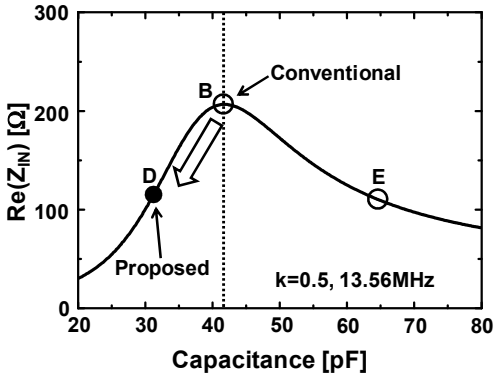

(b)

Fig. 3. Simulated capacitance dependence of (a) θ and (b) Re(Z_{IN}) at k = 0.5 and 13.56MHz.

III. Experimental Results

In order to demonstrate the improvement of η_{TOTAL} by the proposed ZPDCC, a magnetically resonant wireless power transmission system with ZPDCC is implemented. Fig. 4 shows a circuit schematic of the magnetically resonant wireless power transmission system with ZPDCC. The class-D PA in TX and the rectifier in RX are designed and fabricated in a 3.3V, 180nm CMOS process. The coils are fabricated on FR4 PCB and the layout of the coils are the same as [1]. The capacitors are implemented by ceramic capacitors on PCB.

In the circuit implementation of ZPDCC, θ is measured by the phase difference between the voltage (V_1) and the current (I_1) in TX. The proposed ZPDCC includes a current monitor and a capacitance controller. I_1 is converted to a voltage by a non-inverting amplifier and the θ is measured in the capacitance controller. The capacitance controller tunes C in TX and RX to keep $\theta = 0$ at $\Delta\theta / \Delta C > 0$. The non-inverting amplifier is implemented by an operational amplifier (OPA847ID) and two resisters. The gain of amplifier is 1 + (10kΩ / 100Ω) = 40dB.

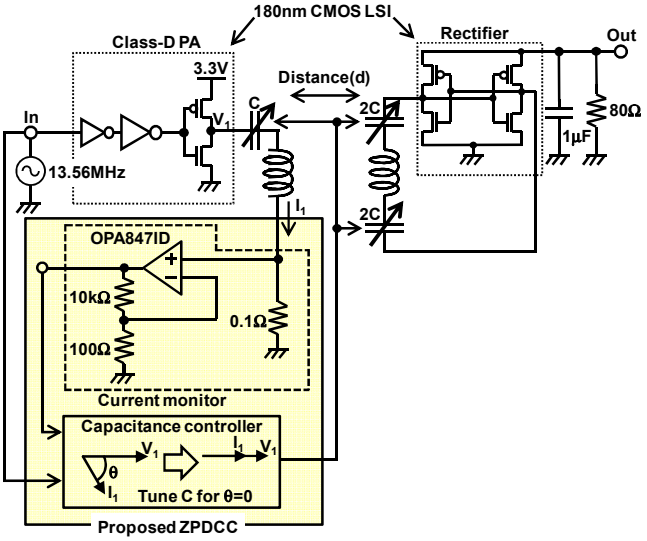

Fig. 4. Circuit schematic of magnetically resonant wireless power transmission system with ZPDCC.

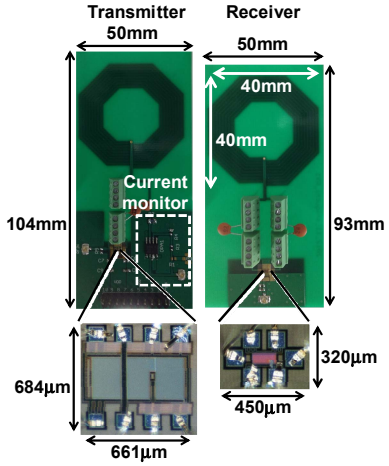

Fig. 5. Photographs of TX PCB, TX LSI (PA), RX PCB, and RX LSI (rectifier).

ZPDCC is achieved by TX, which is important for MR-WPTB, because RX in electronic devices such as smartphones should be simple. Compared with conventional capacitance control methods using a vector network analyzer [4] and a directional coupler and a power meter [5], ZPDCC is suitable for the integration to LSI's, because the current monitor and the capacitance controller are easily implemented into the integrated circuits.

Fig. 5 shows photographs of TX PCB, TX LSI (PA), RX PCB, and RX LSI (rectifier). The size of coils fabricated on TX and RX PCB is 40mm x 40mm. The core size of PA and rectifier is 684μm x 661μm and 320μm x 450μm, respectively.

Fig. 6 shows the measured frequency dependence of η_{TOTAL}, which corresponds to Fig. 1 (e). d is varied. When d = 15mm and 25mm, the frequency dependence of η_{TOTAL} has a one peak at 13.56MHz. In contrast, at d = 5mm, the frequency dependence of η_{TOTAL} has the two peaks. In order to increase η_{TOTAL} at d = 5mm and 13.56MHz, ZPDCC is applied.

Fig. 7 shows the measured capacitance (C) dependence of θ at 13.56MHz, which corresponds to Fig. 3 (a). d is varied. θ is measured with an oscilloscope. When d = 15mm and 25mm, $\theta = 0$ is at only one capacitance, which corresponds to the one peak in Fig. 6. In contrast, at d = 5mm, $\theta = 0$ is at Point B and Point D. Point D is the right point for ZPDCC because Point D satisfies $\theta = 0$ at $\Delta\theta / \Delta C > 0$. Therefore, C should be changed from Point B (C = 37pF) to Point D (C = 25pF).

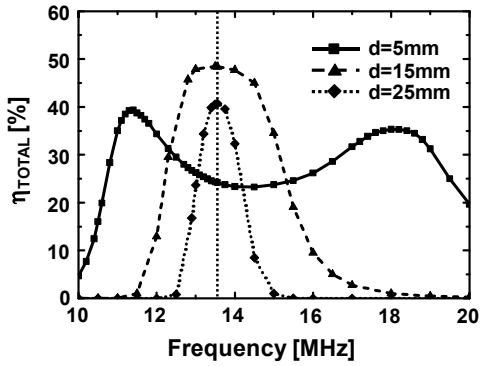

Fig. 6. Measured frequency dependence of η_{TOTAL}, which corresponds to Fig. 1 (e). d is varied.

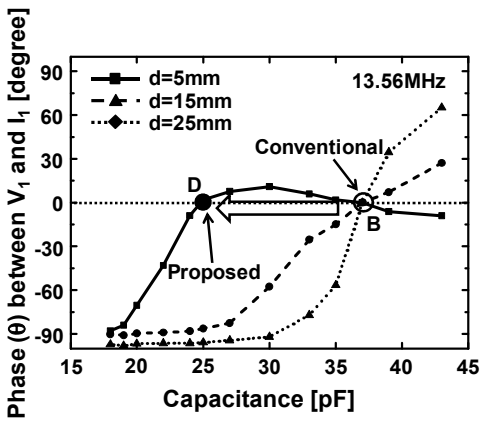

Fig. 7. Measured capacitance dependence of θ at 13.56MHz, which corresponds to Fig. 3 (a). d is varied.

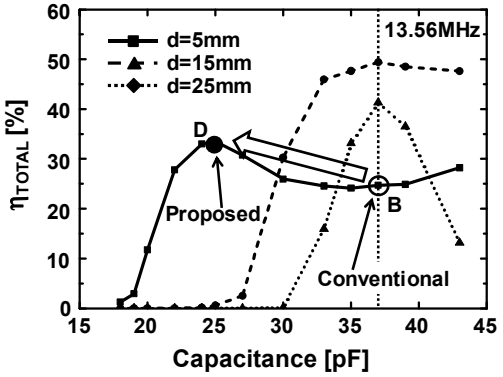

Fig. 8. Measured capacitance dependence of η_{TOTAL} at 13.56MHz. d is varied.

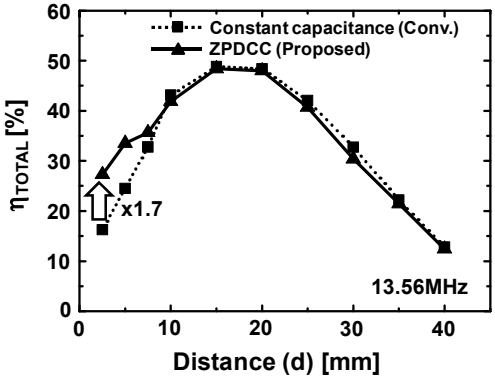

Fig. 9. Measured distance dependence of η_{TOTAL} in conventional constant capacitance and proposed ZPDCC at 13.56MHz.

Fig. 8 shows the measured capacitance (C) dependence of η_{TOTAL} at 13.56MHz. d is varied. When d = 15mm and 25mm, η_{TOTAL} is a maximum at an original C of 37pF. In contrast, at d = 5mm, η_{TOTAL} is a maximum at a modified C of 25pF. η_{TOTAL} is increased from 25% to 34% by changing from Point B (C = 37pF) to Point D (C = 25pF) using ZPDCC. The measured load power (P_4) is 8.4mW at Point D.

Fig. 9 shows the measured distance (d) dependence of η_{TOTAL} at 13.56MHz. The conventional constant C and the proposed ZPDCC are compared.

When d is longer than 10mm, ZPDCC is not activated and C is constant. Therefore, ideally, η_{TOTAL} of ZPDCC and the conventional constant are the same. In the measurement, however, η_{TOTAL} of ZPDCC is 1-7% lower than that of the conventional constant C, because of the resistive loss in 0.1Ω for the current monitor shown in Fig. 4. In contrast, when d is shorter than 10mm, η_{TOTAL} of ZPDCC is higher than that of the conventional constant C, which indicates the increase of η_{TOTAL} by ZPDCC exceeds the decrease of η_{TOTAL} by the resistive loss. For example, η_{TOTAL} increases 1.7 times from 16% to 27% at d = 2.5mm by tuning C from 37pF to 20pF. In ZPDCC, the maximum η_{TOTAL} is 49% at d = 15mm.

IV. Conclusion

For the magnetically resonant wireless power transmission system, ZPDCC is proposed to increase η_{TOTAL} at f_{RES}, when the d is short and η_{TOTAL} at f_{RES} is reduced due to the two peaks. In ZPDCC, C of the resonator is tuned to keep the zero phase difference (θ = 0) between the voltage and the current in TX at $\Delta\theta / \Delta C > 0$, thereby shifting either of the two peaks to f_{RES} and increasing η_{TOTAL}. Compared with the conventional monitoring methods for the capacitance control, the proposed ZPDCC is suitable for the integration to LSI's, because the directional coupler is not required. Both TX circuits and RX circuits are fabricated in a 3.3V, 180nm CMOS. By introducing ZPDCC, the measured η_{TOTAL} at f_{RES} of 13.56MHz increases 1.7 times from 16% to 27% at d = 2.5mm.

Acknowledgment

This work is partly supported by Renesas Electronics Corporation. The authors thank Masayuki Mizuno, Koichi Yamaguchi, Haruya Ishizaki, Hideki Sasaki, Tatsuaki Tsukuda, Hiroki Sugimoto, Yuji Shinohara, and Tomotoshi Nureki of Renesas Electronics Corporation for encouragement and discussions.

The VLSI chips in this study have been fabricated in the chip fabrication program of VLSI Design and Education Center (VDEC), the University of Tokyo in collaboration with Rohm Corporation and Toppan Printing Corporation.

References

[1] H. Lim, K. Ishida, M. Takamiya, and T. Sakurai, "Positioning-Free Magnetically Resonant Wireless Power Transmission Board with Staggered Repeater Coil Array (SRCA)," IEEE MTT-S International Microwave Workshop Series on Innovative Wireless Power Transmission: Technologies, Systems, Applications (IMWS-IWPT), pp. 93-96, May 2012.

[2] I. Awai and T. Ishizaki, "Transferred Power and Efficiency of a Coupled-resonator WPT System," IEEE MTT-S International Microwave Workshop Series on Innovative Wireless Power Transmission: Technologies, Systems, Applications (IMWS-IWPT), pp. 105-108, May 2012.

[3] M. K. Kazimierczuk, RF Power Amplifiers, Wiley, 2008.

[4] K. Ogawa, N. Oodachi, S. Obayashi, and H. Shoki, "A Study of Efficiency Improvement of Wireless Power Transfer by Impedance Matching," IEEE MTT-S International Microwave Workshop Series on Innovative Wireless Power Transmission: Technologies, Systems, Applications (IMWS-IWPT), pp. 155-157, May 2012.

[5] Y. Moriwaki, T. Imura, and U. Hori, "Basic Study on Reduciton of Reflected Power Using DC/DC Converters in Wireless Power Transfer System via Magnetic Resonant Coupling," IEEE 33rd International Telecommunications Energy Conference (INTELEC), pp 1-5, Oct. 2011.